2014 American Control Conference (ACC)
June 4-6, 2014. Portland, Oregon, USA

A Numerical Investigation of Phase and Magnitude Compensation in Adaptive Control of Uncertain Hammerstein Systems with Hysteretic Nonlinearities

Mohammad Al Janaideh and Dennis S. Bernstein

***Abstract*— We apply retrospective cost adaptive control (RCAC) to a command-following problem for uncertain Hammerstein systems with Duhem hysteresis nonlinearities. The only required modeling information of the linear plant is a single Markov parameter. We numerically investigate the sense in which RCAC achieves internal model control. The properties of the asymptotic controller are analyzed by using phase shift calculations.**

I. Introduction

Smart materials, such as piezoelectric ceramics and shape memory alloys, possess the ability to transform current and heat into force and motion without discrete moving parts and thus eliminating stiction and backlash [1]. These materials exhibit hysteretic behavior, which dissipates energy but presents drawbacks when used for precision motion control [1]-[4]. The challenge is thus to develop control algorithms for mechatronic applications that can achieve precise motion control despite the hysteretic behavior.

The most direct approach to overcoming the effects of hysteresis in motion control is to invert a model of the hysteresis nonlinearity. Hysteresis models include Preisach, Prandtl-Ishlinskii, Duhem, and nonlinear feedback [5]-[8], and extensive effort has been devoted to inverting these models [2][4][9][10]. The ability to invert a hysteresis nonlinearity is limited by modeling errors. This uncertainty can be addressed by using controllers that are either robust to the uncertainty or adaptive to changes in the hysteresis [11]-[14].

In the present work we apply retrospective cost adaptive control (RCAC) to linear systems with hysteretic input nonlinearities. To do this, we consider SISO plants with input nonlinearities modeled by Duhem hysteresis. Duhem hysteresis models may be either rate independent or rate dependent, and are used to model magnetic and friction effects [15]-[16].

The specific problem that we consider is a command-following problem with sinusoidal command. When the response of the closed-loop system reaches harmonic steady state, we can analyze the controller performance by examining the magnitude and phase of the converged controller at the command frequency as well as at harmonics introduced by the hysteresis nonlinearity. This analysis allows us to determine whether RCAC converges to an internal model controller for the command signal and its harmonics.

M. Al Janaideh is with the Department of Mechatronics Engineering, The University of Jordan, Amman 11942, Jordan. D. S. Bernstein is with the Department of Aerospace Engineering, The University of Michigan, Ann Arbor, MI 48109.

II. Background

We begin with nonadaptive control for a servo loop with harmonic commands. For a SISO LTI plant, we choose an internal model control law under the assumption that the command frequency is known. Consider the linear system

$$x(k+1) = Ax(k) + Bu(k), \tag{1}$$

$$y(k) = Cx(k), \tag{2}$$

$$z(k) = r(k) - y(k), \tag{3}$$

where $x(k) \in \mathbb{R}^n$ is the state, $y(k) \in \mathbb{R}$ is the measured output available to the controller, $z(k) \in \mathbb{R}$ is the command-following error, $u(k) \in \mathbb{R}$ is the control, and $r(k) \in \mathbb{R}$ is the harmonic command. The goal is to determine u that makes z small.

The closed-loop system in Figure 1 can be represented by the cascaded system in Figure 2, where

$$G_{ur} = \frac{G_c}{1 + G_c G}. \tag{4}$$

Suppose that the system shown in Figure 2 is driven by the command signal $r(k) = \mathrm{Re}\{A_r e^{\jmath\Omega k}\}$, where A_r is a complex number. Then the harmonic control input to the system G can be expressed as

$$u(k) = |G_{ur}(e^{\jmath\Omega})| \mathrm{Re}\{A_r e^{\jmath\left(\Omega k + \angle G_{ur}(e^{\jmath\Omega})\right)}\}, \tag{5}$$

where $|G_{ur}(e^{\jmath\Omega})|$ and $\angle G_{ur}(e^{\jmath\Omega})$ are the gain and phase of

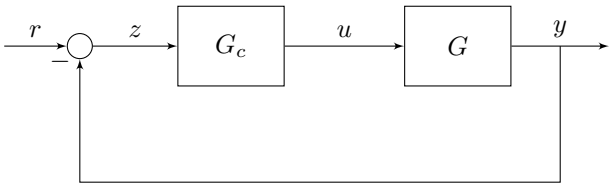

Fig. 1. Command-following problem for the linear plant G with the controller G_c.

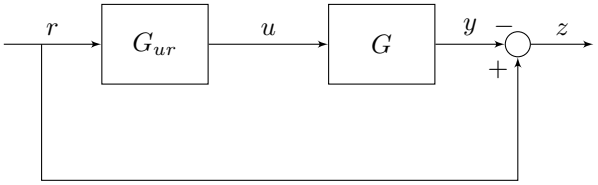

Fig. 2. Representation of the command-following problem as a cascaded system.

978-1-4799-3271-9/$31.00 ©2014 AACC

G_{ur}, respectively. Then

$$y(k) = |G_{ur}(e^{\jmath\Omega})||G(e^{\jmath\Omega})|\mathrm{Re}\big\{A_r e^{\jmath\left[\Omega k+\angle G_{ur}(e^{\jmath\Omega})+\angle G(e^{\jmath\Omega})\right]}\big\}. \tag{6}$$

To regulate the command-following error z to 0 at the frequency Ω, it follows that y is harmonic and $z = 0$ if and only if

$$y(k) = G(e^{\jmath\Omega})G_{ur}(e^{\jmath\Omega})r(k), \tag{7}$$

which is equivalent to

$$G_{ur}(e^{\jmath\Omega})G(e^{\jmath\Omega}) = 1. \tag{8}$$

The gain and phase of G_{ur} therefore must satisfy

$$|G_{ur}(e^{\jmath\Omega})| = \frac{1}{|G(e^{\jmath\Omega})|}, \tag{9}$$

$$\angle G_{ur}(e^{\jmath\Omega}) = -\angle G(e^{\jmath\Omega}). \tag{10}$$

Note that (9) and (10) are satisfied if and only if G_{ur} inverts G at the frequency Ω.

III. Problem Formulation

Consider the Hammerstein command-following problem

$$x(k+1) = Ax(k) + Bv(k), \tag{11}$$

$$y(k) = Cx(k), \tag{12}$$

$$v(k) = \mathcal{N}\big(u(k)\big), \tag{13}$$

$$z(k) = r(k) - y(k), \tag{14}$$

where $x(k) \in \mathbb{R}^n$ is the state, $r(k) \in \mathbb{R}$ is the command, $u(k)$ is the control, $\mathcal{N}\colon \mathbb{R} \to \mathbb{R}$ is the hysteretic nonlinearity, and $z(k)$ is the command-following error. We assume that G is uncertain except for a limited number of Markov parameters. The hysteretic nonlinearity is also uncertain. The Hammerstein system is shown in Figure 3. A block diagram for (11)–(14) is shown in Figure 4. We apply the Hammerstein system in order to have the output y follow the command signal r. The goal is to determine a controller that makes z small.

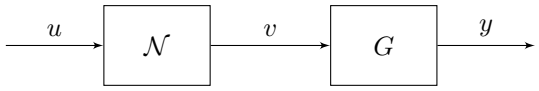

Fig. 3. Hammerstein system with hysteretic nonlinearity $\mathcal{N}$.

IV. The Adaptive Controller

In this section we present the adaptive RCAC controller used in this paper to formulate G_{ur}. Let the controller of order n_c have the form

$$u(k) = \sum_{i=1}^{n_c} M_i(k)u(k-i) + \sum_{i=1}^{n_c} N_i(k)z(k-i), \tag{15}$$

where, for all $i = 1, \ldots, n_c$, $M_i(k) \in \mathbb{R}$, and $N_i(k) \in \mathbb{R}$. The control (15) can be expressed as

$$u(k) = \theta(k)\phi(k-1),$$

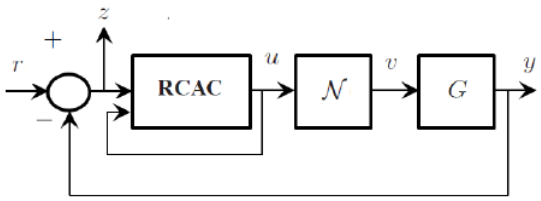

Fig. 4. Adaptive command-following problem for a Hammerstein system. The discrete-time model $\mathcal{N}$ is shown with the RCAC adaptive controller and the linear plant G. We assume that measurements of $z(k)$ are available for feedback; however, measurements of $v(k) = \mathcal{N}\big(u(k)\big)$ and $w(k)$ are not available.

where $\theta(k) \in \mathbb{R}^{\,2n_c}$

$$\theta(k) \triangleq \begin{bmatrix} M_1(k) \cdots M_{n_c}(k) & N_1(k) \cdots N_{n_c}(k) \end{bmatrix}$$

is the controller gain matrix, and the regressor vector $\phi(k) \in \mathbb{R}^{2n_c}$ is given by

$$\phi(k-1) \triangleq [u(k-1) \cdots u(k-n_c) \quad z(k-1) \cdots z(k-n_c)]^{\mathrm{T}}.$$

The transfer function matrix $G_{c,k}(\mathbf{q})$ from z to u at time step k can be represented by

$$\frac{N_1(k)\mathbf{q}^{n_c-1} + N_2(k)\mathbf{q}^{n_c-2} + \cdots + N_{n_c}(k)}{\mathbf{q}^{n_c} - \Big(M_1(k)\mathbf{q}^{n_c-1} + \cdots + M_{n_c-1}(k)\mathbf{q} + M_{n_c}(k)\Big)}.$$

This approach relies on knowledge of Markov parameters. For each example we specify the initial covariance term P_0 and the controller order n_c of the RCAC adaptive controller.

V. Duhem Model

We consider the single-input, single-output Duhem model given by

$$\dot{v}(t) = f(v(t), u(t))g(\dot{u}(t)), \tag{16}$$

$$y(t) = h(v(t), u(t)), \tag{17}$$

where $v : [0, \infty) \to \mathbb{R}^n$ is absolutely continuous, $u : [0, \infty) \to \mathbb{R}$ is continuous and piecewise C^1, $f : \mathbb{R}^n \times \mathbb{R} \to \mathbb{R}^{n\times r}$ is continuous, $g : \mathbb{R} \to \mathbb{R}^r$ is continuous and satisfies $g(0) = 0$, $y : [0, \infty) \to \mathbb{R}$, and $h : \mathbb{R}^n \times \mathbb{R} \to \mathbb{R}$ is continuous. The properties of (16) are discussed in [8]. We review the following properties for the Duhem model: (i) the rate-dependence of the Duhem model, and (ii) discontinuity of $g(\dot{u}(t))$ at $\dot{u}(t) = 0$.

We can show that if $g(\dot{u}(t)) = |\dot{u}(t)|$ then the Duhem model is rate-independent. Following [8], let τ be a positive time scale. Then $\dot{\tau} > 0$ and $\tau(0) = 0$ and, thus, $v_\tau(0) = v(\tau(0)) = v(0) = v_0$. Now, for all $t > 0$, consider

$$\frac{\mathrm{d}v_\tau(t)}{\mathrm{d}t} = f(v_\tau(t), u_\tau(t))|\frac{\mathrm{d}u_\tau(t)}{\mathrm{d}t}|. \tag{18}$$

Then,

$$\frac{\mathrm{d}v(\tau(t))}{\mathrm{d}t} = f\left(v(\tau(t)), u(\tau(t))\right)|\frac{\mathrm{d}u(\tau(t))}{\mathrm{d}t}|,$$

$$\dot{\tau}\frac{\mathrm{d}v(\tau)}{\mathrm{d}\tau} = f\left(v(\tau), u(\tau)\right)|\dot{\tau}\frac{\mathrm{d}u(\tau)}{\mathrm{d}\tau}|,$$

and

$$\dot{\tau}\frac{\mathrm{d}v(\tau)}{\mathrm{d}\tau} - f\left(v(\tau),u(\tau)\right)|\dot{\tau}\frac{\mathrm{d}u(\tau)}{\mathrm{d}\tau}| = 0.$$

Then,

$$\dot{\tau}\left[\frac{\mathrm{d}v(\tau)}{\mathrm{d}\tau} - f\left(v(\tau),u(\tau)\right)|\frac{\mathrm{d}u(\tau)}{\mathrm{d}\tau}|\right] = 0. \tag{19}$$

Following Madelung's hysteresis model [18], the Duhem model can be expressed as

$$\dot{v}(t) = \begin{cases} f_+(v(t),u(t))g(\dot{u}(t)), & \text{if} \quad \dot{u}(t) \geq 0 \quad \text{increases}, \\ f_-(v(t),u(t))g(\dot{u}(t)), & \text{if} \quad \dot{u}(t) \leq 0 \quad \text{decreases}. \end{cases} \tag{20}$$

If g is continuous at $\dot{u}(t) = 0$, $f_+(v(t),u(t)) = f_-(v(t),u(t))$, the positive and negative curves of the Duhem model are identical and thus the periodic input-output map is not hysteretic. Therefore, a necessary condition for (32) to be hysteretic is that g have a slope discontinuous at $\dot{u}(t) = 0$.

A. the sampled-data Duhem hysteresis model

We consider the sampled-data Duhem hysteresis model

$$\dot{v}(t) = \kappa_1|\dot{u}(t)|(\kappa_2 u(t) - v(t)) + \kappa_3\dot{u}(t), \tag{21}$$

where the positive constants κ_1, κ_2, and κ_3 determine the shape and the area of the hysteresis loop. The model (21) is implemented using Simulink with sampling time T_s. The sampled-data Duhem model can be expressed as

$$\dot{v}(t) = \begin{cases} \left[\kappa_1(\kappa_2 u(t) - v(t)) + \kappa_3\right]|\dot{u}(t)|, & \text{if} \quad u(t) \quad \text{increases}, \\ \left[\kappa_1(\kappa_2 u(t) - v(t)) - \kappa_3\right]|\dot{u}(t)|, & \text{if} \quad u(t) \quad \text{decreases}. \end{cases} \tag{22}$$

Then,

$$f(v(t),u(t)) = \begin{cases} \left[\kappa_1(\kappa_2 u(t) - v(t)) + \kappa_3\right], & \text{if} \quad u(t) \quad \text{increases}, \\ \left[\kappa_1(\kappa_2 u(t) - v(t)) - \kappa_3\right], & \text{if} \quad u(t) \quad \text{decreases}, \end{cases} \tag{23}$$

and

$$g(\dot{u}(t)) = |\dot{u}(t)|. \tag{24}$$

This model presents the relationship between the magnetic field strength and the magnetic flux density of a ferromagnetically soft material of the isoperm type [17].

VI. The Phase Shift

In this section, we use the phase shift between the command input $r(k)$ and the output $y(k)$ and the command-following error $z(k)$ to investigate whether RCAC inverts the Hammerstein system that consists of the linear plant $G(z)$ and the sampled-data Duhem hysteresis model (21). We consider the magnitude and phase shift of the most significant harmonic component in the output $v(k)$. The output of the sampled-data Duhem model hysteresis model can be approximated by

$$v(k) \cong \mathrm{Re}\big\{A_u e^{\jmath(\Omega k+\psi)}\big\}, \tag{25}$$

where ψ represents the phase of the most significant harmonic component in the output $v(k)$. Then, the harmonic steady-state response for the Hammerstein system with the sampled-data Duhem model hysteresis model is given by

$$y(k) \cong \mathrm{Re}\big\{A_r A_u|G(e^{\jmath\Omega})|e^{\jmath(\Omega k+\angle G(e^{\jmath\Omega})+\psi)}\big\}. \tag{26}$$

Therefore, $z(k) \cong 0$ if and only if the magnitude and phase of $G_{ur}(e^{\jmath\Omega})$ satisfy

$$|G_{ur}(e^{\jmath\Omega})| \cong \frac{1}{A_r|G(e^{\jmath\Omega})|}, \tag{27}$$

$$\angle G_{ur}(e^{\jmath\Omega}) \cong -\angle G(e^{\jmath\Omega}) - \psi. \tag{28}$$

To examine the phase shift between $\angle G_{ur}(e^{\jmath\Omega})$ and $\angle G(e^{\jmath\Omega}) + \psi$, we use the fourier transform to determine the most significant frequency component in the signal. Then, we calculate the phase of the most significant frequency component of the two signals. Finally, by using two periods at steady state we compute the phase difference between the two signals.

VII. Numerical Examples

A. Closed-loop system with $\mathcal{N}(u) = u$

In this section we consider the hammerstein system without the hysteresis nonlinearity for the command-following problem (1)–(3).

Example 7.1: We use the command signal $r(k) = 1\sin(\omega k)$, where $\omega = \frac{\pi}{5}$ rad/sample. We let $n_{\mathrm{c}} = 30$ and $P_0 = 0.1I_{2n_{\mathrm{c}}}$. We consider the linear stable plant $G(z) = \frac{1}{z-0.5}$ and linear unstable plant $G(z) = \frac{1}{z-1.1}$. Figure 5 shows the simulation results. The results show that RCAC stabilizes the closed-loop system and decreases the command-following error z for the harmonic command r. It remains to be shown that G_{ur} obtained from RCAC inverts the linear plants at the command frequency. The phase shift between the control signal $u(k)$ and the output $y(k)$ is 3.512°, and the phase shift between the reference input $r(k)$ and the control signal $u(k)$ is -3.515°. With $G(z) = \frac{1}{z-1.1}$, the phase shift between the control signal $u(k)$ and the output $y(k)$ is 163.196°, and the phase shift between the reference input $r(k)$ and the control signal $u(k)$ is -163.018°. ■

B. Closed-loop system with $G(z) = 1$

In this section we consider the Hammerstein system without the linear plant $G(z)$. We consider the Duhem model (21)

We consider command-following problem

$$v(k) = \mathcal{N}\big(u(k)\big), \tag{29}$$

$$y(k) = v(k), \tag{30}$$

$$z(k) = r(k) - y(k). \tag{31}$$

Example 7.2: We consider the sampled-data Duhem hysteresis model with $\kappa_1 = 1$, $\kappa_2 = 2$, and $\kappa_3 = 1$. We use the command signal $r(k) = 4\sin(2\omega k) + \sin(\omega k)$, where $\omega = \frac{\pi}{10}$ rad/sample to show major and minor hysteresis loops. We let $n_{\mathrm{c}} = 30$ and $P_0 = 0.1I_{2n_{\mathrm{c}}}$. Figure 7 shows the simulation results. The results show that RCAC stabilizes the

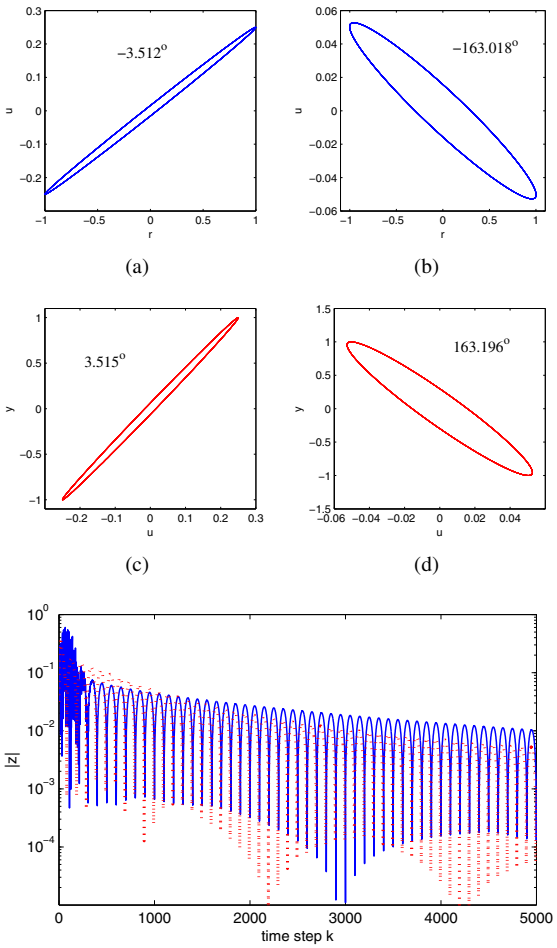

Fig. 5. Example 7.1. (a) and (b) shows $r(k)$ versus $u(k)$ with (a) $G(z) = \frac{1}{z-0.5}$, and (b) $G(z) = \frac{1}{z-1.1}$ when $r(k) = \sin(\omega k)$, where $\omega = \frac{\pi}{10}$ rad/sample. (c) and (d) shows $u(k)$ versus $y(k)$ when $r(k) = \sin(\omega k)$, where $\omega = \frac{\pi}{10}$ rad/sample, with (c) $G(z) = \frac{1}{z-0.5}$, and (d) $G(z) = \frac{1}{z-1.1}$ when $r(k) = \sin(\omega k)$, where $\omega = \frac{\pi}{10}$ rad/sample. (e) shows the closed-loop response with $G(z) = \frac{1}{z-0.5}$ (dotted line), and $G(z) = \frac{1}{z-1.1}$ (dashed line).

closed-loop system and decreases the command-following error z for the harmonic command r. It remains to be shown that G_{ur} obtained from RCAC inverts the sampled-data Duhem hysteresis model at the command frequency. The phase shift between the control signal $u(k)$ and the output $y(k)$ is $13.405°$, and the phase shift between the reference input $r(k)$ and the control signal $u(k)$ is $-13.671°$. In order to consider hysteresis nonlinearity with saturation, let

$$f(v, u) = \tanh(2u) - v \tag{32}$$

and

$$g(\dot{u}(t)) = |\dot{u}(t)|. \tag{33}$$

Figure 7 shows the simulation results. The results show that RCAC stabilizes the closed-loop system and decreases the command-following error z for the harmonic command r. It remains to be shown that G_{ur} obtained from RCAC inverts the sampled-data Duhem hysteresis model with 32 at the command frequency. The phase shift between the control signal $u(k)$ and the output $y(k)$ is $8.401°$, and the phase shift between the reference input $r(k)$ and the control signal $u(k)$ is $-8.124°$. ■

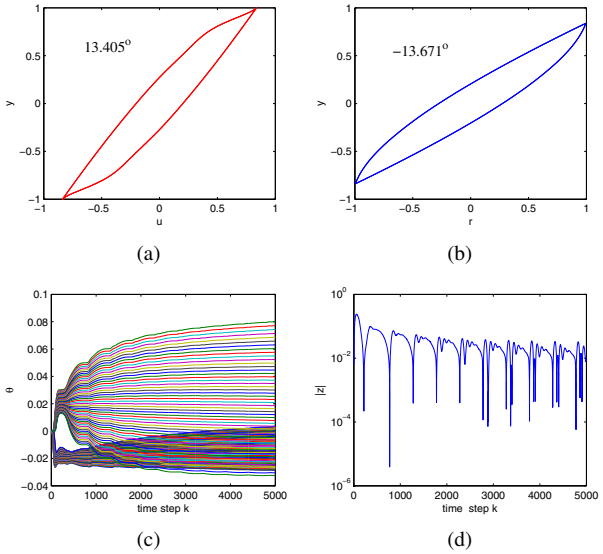

Fig. 6. Example 7.2. (a) shows the output of the sampled-data Duhem hysteresis model and the command signal $r(k) = \sin(\omega k)$, where $\omega = \frac{\pi}{10}$ rad/sample, (b) shows the relationship between the command signal $r(k)$ and the control signal $u(k)$, (c) shows the evolution of the controller coefficients θ, (d) shows the closed-loop response to the command signal $r(k) = \sin(\omega k)$, where $\omega = \frac{\pi}{10}$ rad/sample.

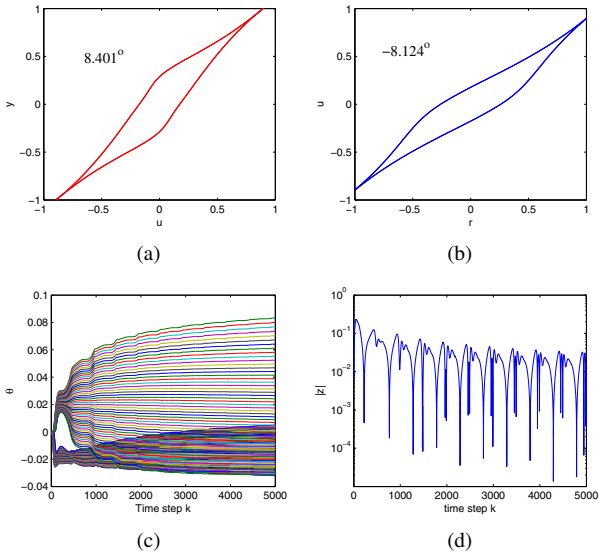

Fig. 7. Example 7.2. (a) shows the output of the sampled-data Duhem hysteresis model and the command signal $r(k) = \sin(\omega k)$, where $\omega = \frac{\pi}{10}$ rad/sample, (b)shows $r(k)$ versus $u(k)$ with, (c) shows the evolution of the controller coefficients θ, (d) shows the closed-loop response to the command signal $r(k) = \sin(\omega k)$, where $\omega = \frac{\pi}{10}$ rad/sample.

C. Closed-loop system with Duhem input nonlinearity

Example 7.3: We consider the sampled-data Duhem hysteresis model with $\kappa_1 = 1$, $\kappa_2 = 2$, and $\kappa_3 = 1$ and

the linear plants $G(z) = \frac{1}{z-0.5}$ and $G(z) = \frac{1}{z-1}$. We use the command signal $r(k) = 4\sin(2\omega k)+\sin(\omega k)$, where $\omega = \frac{\pi}{10}$ rad/sample. We let $n_c = 30$ and $P_0 = 0.1I_{2n_c}$. Figure 8 shows the simulation results with $G(z) = \frac{1}{z-0.5}$. The results show that RCAC stabilizes the closed-loop system and decreases the command-following error z for the harmonic command r. It remains to be shown that G_{ur} obtained from RCAC inverts the sampled-data Duhem hysteresis model at the command frequency.

The phase shift between the control signal $u(k)$ and the output $y(k)$ is $14.524°$, and the phase shift between the reference input $r(k)$ and the control signal $u(k)$ is $-14.437°$. Figure 9 shows the simulation results with $G(z) = \frac{1}{z-1}$. The phase shift between the control signal $u(k)$ and the output $y(k)$ is $90.739°$, and the phase shift between the reference input $r(k)$ and the control signal $u(k)$ is $-90.591°$. ■

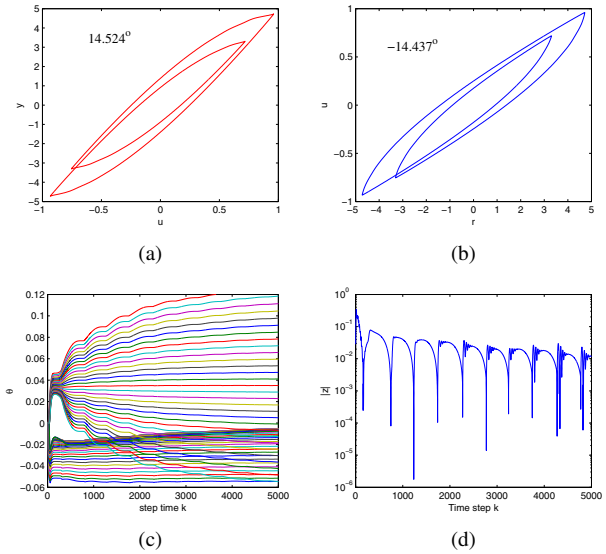

(a) (b) (c) (d)

Fig. 8. Example 7.3. (a) shows the output of the sampled-data Duhem hysteresis model and the command signal $r(k) = \sin(\omega k)$, where $r(k) = 4\sin(2\omega k) + \sin(\omega k)$, where $\omega = \frac{\pi}{10}$ rad/sample, (b) shows $r(k)$ versus $u(k)$, (c) shows the evolution of the controller coefficients θ, (d) shows the closed-loop response to the command signal $r(k) = \sin(\omega k)$, where $r(k) = 4\sin(2\omega k) + \sin(\omega k)$, where $\omega = \frac{\pi}{10}$ rad/sample.

Example 7.4: We consider the sampled-data Duhem hysteresis model with $\kappa_1 = 1$, $\kappa_2 = 2$, and $\kappa_3 = 1$ and

$$f(u, v) = \tanh(4u) - v, \tag{34}$$

$$g(\dot{u}) = |\dot{u}(t)|, \tag{35}$$

and the linear plants $G(z) = \frac{1}{z-0.8}$ and $G(z) = \frac{z-0.7}{(z-0.8)(z-0.5)}$. We use the command signal $r(k) = 4\sin(2\omega k) + \sin(\omega k)$, where $\omega = \frac{\pi}{10}$ rad/sample. We let $n_c = 50$ and $P_0 = 0.01I_{2n_c}$. Figure 10 shows the simulation results for the closed-loop system with $G(z) = \frac{1}{z-0.8}$. The phase shift between the control signal $u(k)$ and the output $y(k)$ is $24.272°$, and the phase shift between the reference input $r(k)$ and the control signal $u(k)$ is $-24.189°$.

Figure 12 shows the simulation results for the closed-loop system with $G(z) = \frac{z-0.7}{(z-0.8)(z-0.5)}$. The phase shift

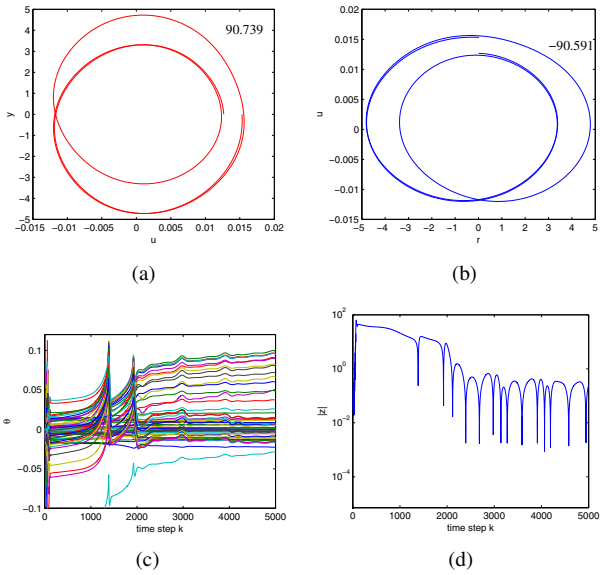

(a) (b) (c) (d)

Fig. 9. Example 7.3. (a) shows the output of the sampled-data Duhem hysteresis model and the command signal $r(k) = \sin(\omega k)$, where $r(k) = 4\sin(2\omega k) + \sin(\omega k)$, where $\omega = \frac{\pi}{10}$ rad/sample, (b) shows $r(k)$ versus $u(k)$, (c) shows the evolution of the controller coefficients θ, (d) shows the closed-loop response to the command signal $r(k) = \sin(\omega k)$, where $\omega = \frac{\pi}{2}$ rad/sample.

between the control signal $u(k)$ and the output $y(k)$ is $17.355°$, and the phase shift between the reference input $r(k)$ and the control signal $u(k)$ is $-17.285°$.Figure 12 shows the simulation results for the closed-loop system with $G(z) = \frac{1}{z-1.05}$. The phase shift between the control signal $u(k)$ and the output $y(k)$ is $172.423°$, and the phase shift between the reference input $r(k)$ and the control signal $u(k)$ is $-172.439°$. ■

VIII. CONCLUSIONS

Retrospective cost adaptive control (RCAC) was applied to a command-following problem involving hysteresis nonlinearities characterized by the Duhem model. RCAC was used with limited modeling information about the plant. The numerical investigation in the paper shows that RCAC can achieve internal model control of Hammerstein systems with an unknown input hysteresis nonlinearity.

REFERENCES

[1] R. C. Smith, *Smart Material Systems*, Philadelphia, Springler-Verlag, 2005.

[2] P. Krejčí and K. Kuhnen, "Inverse control of systems with hysteresis and creep," *IEE Proc. Contr. Theo. Appl.*, vol. 148, pp. 185-192, 2001.

[3] J. Cruz-Hernandez and V. Hayward, "Phase control approach to hysteresis reduction," *IEEE Trans. Contr. Sys. Tech.*, vol. 9, pp.17-26, 2001.

[4] M. Al Janaideh and P. Krejci, "Inverse rate-dependent PrandtlIshlinskii model for feedforward compensation of fysteresis in a piezomicropositioning actuator," *IEEE/ASME Trans. Mech.*, vol. 18, pp. 1498-1507, 2013.

[5] M. Brokate and J. Sprekels, *Hysteresis and Phase Transitions*, Springer, Berlin, 1996.

[6] I. Mayergoyz, *Mathematical Models of Hysteresis*, Elsevier, New York, 2003.

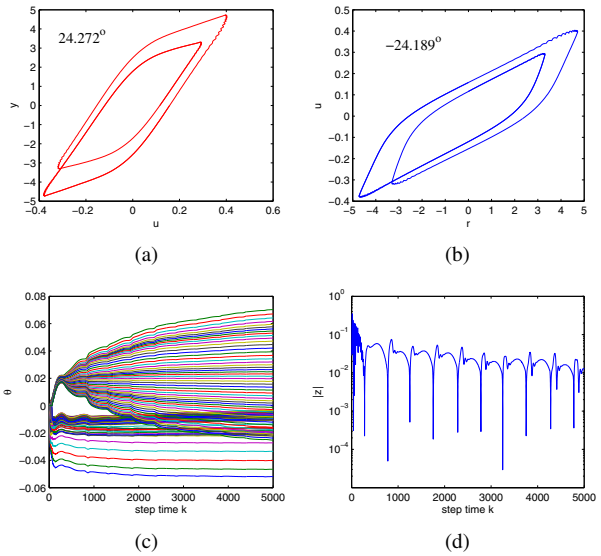

Fig. 10. Example 7.4. (a) shows the output of the sampled-data Duhem hysteresis model with $f(u,v) = \tanh(4u) - v$ and the command signal $r(k) = \sin(\omega k)$, where $r(k) = 4\sin(2\omega k) + \sin(\omega k)$, where $\omega = \frac{\pi}{10}$ rad/sample, (b) shows $r(k)$ versus $u(k)$, (c) shows the evolution of the controller coefficients θ, (d) shows the response of the closed-loop system with with $G(z) = \frac{z-0.7}{(z-0.8)(z-0.5)}$ and $r(k) = 4\sin(2\omega k) + \sin(\omega k)$, where $\omega = \frac{\pi}{10}$ rad/sample.

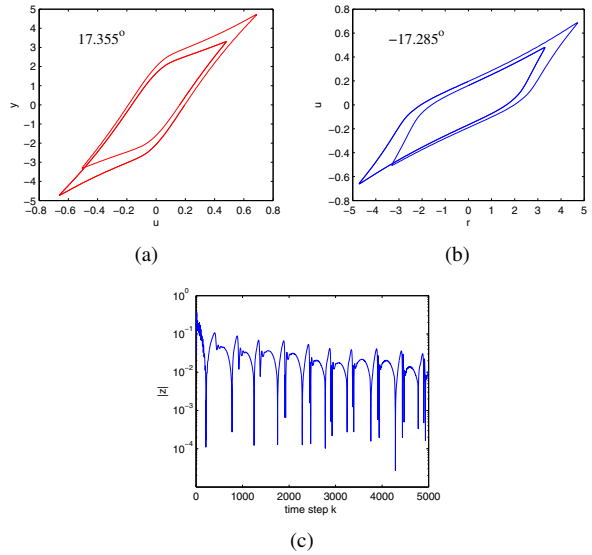

Fig. 11. Example 7.4. (a) shows the output of the sampled-data Duhem hysteresis model with $f(u,v) = \tanh(4u) - v$ and the command signal $r(k) = \sin(\omega k)$, where $r(k) = 4\sin(2\omega k) + \sin(\omega k)$, where $\omega = \frac{\pi}{10}$ rad/sample, (b) shows $r(k)$ versus $u(k)$, (c) shows the response of the closed-loop system with with $G(z) = \frac{1}{z-0.8}$ and $r(k) = 4\sin(2\omega k) + \sin(\omega k)$, where $\omega = \frac{\pi}{10}$ rad/sample.

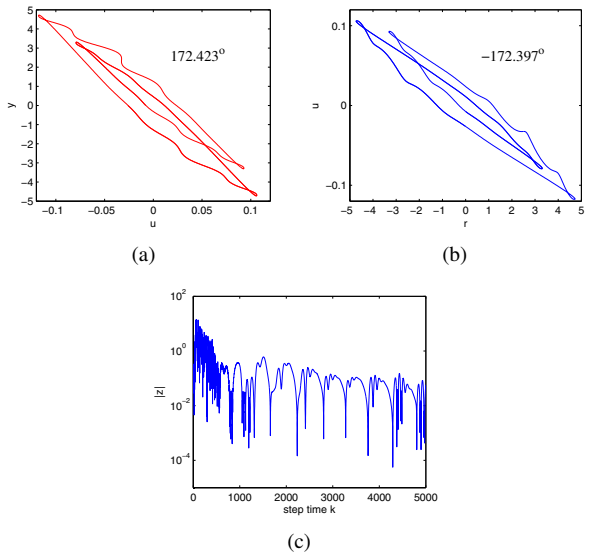

Fig. 12. Example 7.4. (a) shows the output of the sampled-data Duhem hysteresis model with $f(u,v) = \tanh(4u) - v$ and the command signal $r(k) = \sin(\omega k)$, where $r(k) = 4\sin(2\omega k) + \sin(\omega k)$, where $\omega = \frac{\pi}{10}$ rad/sample, (b) shows $r(k)$ versus $u(k)$, (c) shows the response of the closed-loop system with with $G(z) = \frac{1}{z-1.05}$ and $r(k) = 4\sin(2\omega k) + \sin(\omega k)$, where $\omega = \frac{\pi}{10}$ rad/sample.

[7] J. Oh, B. Drincic, and D. S. Bernstein, "Nonlinear feedback models of hysteresis: backlash, bifurcation, and multistability," *IEEE Contr. Sys. Mag.*, vol. 29, pp. 100-119, 2009.

[8] J. Oh and D. S. Bernstein, "A semilinear Duhem model for rate-independent and rate-dependent hysteresis," *IEEE Trans. Autom. Contr.*, vol. 50, pp. 631-645, 2005.

[9] M. Al Janaideh and P. Krejci, "Prandtl-Ishlinskii hysteresis models for complex time dependent hysteresis nonlinearities," *Physica B*, vol. 407, pp. 1365-1367, 2012.

[10] R. C. Smith, "Inverse compensation for hysteresis in magnetostrictive transducers," *Math. and Comp. Model.*, vol. 33, pp. 285-298, 2001.

[11] M. Al Janaideh, "About the output of the inverse compensation of the Prandtl-Ishlinskii model," *Proc. Amer. Contr. Conf.*, pp. 247-252, Washington, DC, June 2013.

[12] P. Ge and M. Jouaneh, "Tracking control of a piezoceramic actuator," *IEEE Trans. Contr. Sys. Tech.*, vol. 4, pp. 209-216, 1996.

[13] X. Fan and R. C. Smith, "Model-based $\mathcal{L}1$ adaptive control of hysteresis in smart materials," *Proc. Conf. Dec. Contr.*, Cancun, Mexico, pp. 3251-3256, 2008.

[14] X. Tan and H. Khalil, "Control unknown dynamic hysteretic systems using slow adaption: preliminary results," *Proc. Amer. Contr. Conf.*, NewYork, NY, pp. 3294- 3299, 2007.

[15] J. Oh and D. S. Bernstein, "A semilinear Duhem model for rate-independent hysteresis," *Proc. Conf. Dec. Contr.*, pp. 6236-6241, Maui, HI, Dec. 2003.

[16] J. Oh, A. Padthe, D. S. Bernstein, D. Rizos, and S. D. Fassois, "Duhem models for hysteresis in sliding and presliding friction," *Proc. Conf. Dec. Contr.*, pp. 8132-8137, Seville, Spain, Dec. 2005.

[17] B. Coleman and M. Hodgdon, "A constitutive relation for rateindependent hysteresis in ferromagnetically soft materials," *Int. J. Eng. Sci.*, vol. 24, pp. 897-919, 1986.

[18] M. Krasnoselskii and A. Pokrovskii, *Systems with Hysteresis*, New York: Springer-Verlarg, 1989.

[19] R. Venugopal and D. S. Bernstein, "Adaptive disturbance rejection using ARMARKOV system representations," *IEEE Trans. Contr. Sys. Tech.*, vol. 8, pp. 257-269, 2000.

[20] J. B. Hoagg, M. A. Santillo and D. S. Bernstein, "Discrete-time adaptive command following and disturbance rejection for minimum-phase systems with unknown exogenous dynamics," *IEEE Trans. Autom. Contr.*, vol. 53, pp. 912-928, 2008.

[21] M. A. Santillo and D. S. Bernstein, "Adaptive control based on retrospective cost optimization," *AIAA J. Guid. Contr. Dyn.*, vol. 33, pp. 289-304, 2010.

[22] M. Al Janaideh, D. Sumer, J. Yan, A. M. D'Amato, B. Drincic, K. Aljanaideh, and D. S. Bernstein, "Adaptive Control of Uncertain Hammerstein Systems with Uncertain Hysteretic Input Nonlinearities," *Proc. Dyn. Sys. and Contr. Conf.* , Fort Lauderdale, FL, October 2012, DSCC2012-MOVIC2012-8573, pp. 1-10.